ALBEDO INFLUENCE ON THE PERFORMANCE OF SOLAR TRANSPOSITION MODELS

Inti Piccioli[1], Agustín Laguarda[1] and Gonzalo Abal[2]

[1] Laboratorio de Energía Solar/Instituto de Física, Facultad de Ingeniería, Universidad de la República - Montevideo (Uruguay)

[2] Laboratorio de Energía Solar, Departamento de Fïsica, Cenur Litoral Norte, Universidad de la República - Salto (Uruguay)

Abstract

Accurately estimating solar irradiance on tilted surfaces is essential for the performance assessment and optimization of solar energy systems. This work evaluates the accuracy and sensitivity to surface albedo assumptions of five widely used transposition models when estimating solar irradiance on tilted surfaces. Using high quality data from a site in Golden, Colorado, we assess model performance for the diffuse component of global tilted irradiance (GTI), defined as the sum of in-plane and reflected irradiance on the tilted surface by calculating the relative mean bias deviation (rMBD), the relative root mean square deviation (rRMSD), and the combined metric U_{95}. Then we evaluate sensitivity and robustness of the models for different surface albedo choices. Results indicate that the Hay-Davies and Reindl models exhibit greater robustness to variations in albedo, maintaining consistent accuracy, while the Perez and Temps-Coulson-Klucher models are more sensitive to inaccurate albedo assumptions. However, these two models are the most accurate when the true measured albedo is used. The isotropic assumption for the diffuse component (referred to as the isotropic model), while robust, systematically underestimates GTI and is therefore not recommended for precise aplications.

Keywords: tilted solar irradiance, global horizontal irradiance, surface albedo, transposition models, solar resource assessment,

1. Introduction

An accurate estimation of solar global irradiance on equator-oriented tilted surfaces (GTI) is essential for the design, performance assessment, and optimization of solar energy systems, including photovoltaic (PV) installations, solar thermal collectors and daylighting applications. Uncertainties and biases in GTI estimation propagate directly into the predicted energy yield of PV systems; thus, inaccurate modeling of GTI increases the financial risk in a project affecting long-term investment decisions.

Since most ground-based radiometric networks measure global solar irradiance on a horizontal plane (GHI), transposition models are required to estimate GTI from its horizontal component. The same applies to satellite-based estimations, which are usually available on a horizontal surface. The direct component of the incident irradiance can be geometrically projected on a tilted plane of any orientation. However, the diffuse component is not trivially transported from horizontal to a tilted surface. In particular, the ground-reflected contribution to diffuse plays an important role, especially for surfaces with high tilt angles and high surface albedo sites, where the reflected irradiance can account for a significant fraction of the total received energy by the tilted plane. An accurate characterization of the diffuse component depends not only on the distribution of diffuse irradiance on the sky (and thus on cloud type and distribution), but also on the surrounding landscape (usually assumed as an horizontal infinite plane) and its surface albedo. These aspects are relevant for a reliable GTI modeling, system yield estimation, and for understanding performance under conditions such as snow or bright ground surfaces.

The key parameter that influences the ground-reflected component of GTI is the hemispherical surface albedo in the shortwave spectral range, also referred to as surface hemispherical reflectance. It is defined as the fraction of GHI that is reflected by the ground. For modeling purposes, the ground is typically assumed

to behave as a Lambertian (perfectly diffuse) reflector, meaning it reflects indicent radiation uniformly in all directions. The horizontal albedo can be measured with two pyranometers facing opposite directions; one facing upward to record the incident GHI and the other facing downward to measure the upwelling irradiance reflected from the ground. This measurement is not usually available at most sites measuring GHI; consequently, the site albedo is often assumed constant, usually between 0.20 and 0.25 for grass or unpainted concrete. While its influence on model accuracy is recognized, few studies have examined how deviations from the actual albedo affect the accuracy of GTI estimates. A recent exception is Tuomiranta et al., 2021. This gap is particularly relevant under snow conditions, where albedo values can exceed 0.8, yet to the best of our knowledge, very few works have explicitly addressed their impact on transposition models. Moreover, Gueymard (2008) emphasized how data quality and representativeness, ranging from optimal to poor conditions, strongly influence GTI estimation.

In this work, we address this issue by evaluating the robustness of five widely used transposition models to deviatons in the albedo assumption. These models differ in how the diffuse component is modeled, and cover a range of complexity: from the simplest Isotropic model (ISO), the Hay–Davies (HD) and Reindl (HDKR) models, which ignore anisotropy (ISO) or deal with diffuse anisotropy in a simplified way (HD and HDKR), to the more sophisticated Perez (PER) and Temps–Coulson–Klucher (TCK) models, which attempt to model the distribution of diffuse irradiance in the sky. An extensive assessment of transposition models, including these ones, was performed by Yang (2016).

Using data from the National Renewable Energy Laboratory (NREL) at its Golden, Colorado (United States) site, which includes measured albedo, we assess the model's performance and their sensitivity to albedo assumptions, aiming to identify which models combine acceptable performance with resilience to albedo uncertainty.

2. Transposition models

The global tilted irradiance (GTI or G_t) received by a plane surface facing towards the equator and inclined an angle β with respect to the horizontal, is the sum of the direct, diffuse, and ground-reflected components

$$G_t = G_{bn}\cos\theta_i + G_{dh}r_d + G_h\rho_g\frac{1-\cos\beta}{2} \qquad \text{(eq. 1)}$$

These three terms of GTI are derived from the global horizontal irradiance (GHI, G_h) and its beam (DNI, G_{bn}) and diffuse (DHI, G_{dh}) components, combined with assumptions about the distribution of the diffuse sky irradiance and the reflection properties of the surrounding elements.

The beam component, $G_{bn}\cos\theta_i$ is obtained by projecting G_{bn} onto the tilted plane, where θ_i is the incidence angle of the solar beam on the surface (dependent only on the site location, time, and surface orientation). The ground-reflected term, $G_h\rho_g(1 - \cos\beta)/2$, assumes isotropic reflection from the ground, where ρ_g is the ground albedo or reflectance, and neglects contribution from any other reflective surfaces nearby other than the ground. The diffuse in-plane irradiance, $G_{dh}r_d$, is expressed by means of the transposition factor r_d, which encapsulates the assumed angular distribution of diffuse sky irradiance. This component is usually the main unknown when estimating GTI and different models propose alternative expressions for r_d based on different approaches. Table 1 summarizes the expressions of r_d for the five transposition models considered in this study, together with references to the original works.

The baseline model is the isotropic assumption (ISO), meaning the diffuse irradiance is uniformly distributed across the sky dome, so r_d reduces to the sky view factor, $(1 + \cos\beta)/2$. It performs reasonably under overcast skies but neglects anisotropies such as circumsolar and horizon brightening (two regions in the sky dome that radiate more intensely than the rest), leading to GTI underestimation in clear-sky conditions. The Hay-Davies (HD) model separates the diffuse in-plane irradiance into an anisotropic circumsolar component, proportional to beam transmittance $\tau_b = \cos\theta_i / \cos\theta_z$,(where θ_z is the solar zenith angle) and an isotropic remainder. It reduces to ISO when $\tau_b=0$, and under clear skies accounts for strong circumsolar contributions, thus reducing the underestimation of the ISO. Simple yet effective, is among the most recommended models in solar engineering practice (Duffie and Beckman, 2013). The Temps-Coulson-Klucher (TCK) model extends the ISO by introducing empirical correction factors for the circumsolar and horizon-brightening

regions observed by Temps and Coulson (1977). A modulation factor $F=1-f_d$, where f_d =DHI/GHI is the diffuse fraction, adjusts between overcast (F=0, reducing to ISO) and clear-sky (F→1) conditions. By capturing key anisotropies, this is one of the best-performing transposition models, while retaining relative simplicity. The Hay-Davies-Klucher-Reindl (HDKR) model combines the HD treatment of circumsolar radiation with the TCK correction for horizon brightening, modulated by Klucher's empirical factor. This hybrid retains simplicity while capturing key anisotropic effects, and has been shown to perform very similarly to HD, making it a robust and widely adopted option. The Perez model (PER) partitions the sky dome into isotropic, circumsolar, and horizon brightening components, parameterized by empirical factors F1 and F2 linked to the sky clearness index ε. Its final 1990 formulation, validated across multiple sites and orientations, remains the most refined and widely accepted transposition model, offering high accuracy under diverse atmospheric conditions.

The ISO, HD, TCK, and HDKR models form a natural hierarchy of progressively refined approaches that retain the structure and simplicity of the isotropic assumption. In contrast, the PER model introduces a geometric partition of the sky dome to account for diffuse anisotropy, representing a higher level of complexity and sophistication, with several empirically derived parameters.

Table 1: Summary of the transposition models evaluated in this work, together with their references and remarks.

Model	diffuse factor r_d	Reference
ISO	$r_d^{ISO}=(1+\cos\beta)/2$	Liu and Jordan, 1961
HD	$r_d^{ISO}+\tau_b r_b$	Hay and Davies, 1980
HDKR	$(1-\tau_b)r_d^{ISO}[1-f'\sin^3(\beta/2)]+\tau_b r_b$	Reindl et al. 1990
TCK	$r_d^{ISO}(1+F\cos^2\theta_i\sin^3\theta_z)[1+F\sin^3(\beta/2)]$	Temps and Coulson, 1977. Klucher, 1979
PER	$(1-F_1)r_d^{ISO}+F_1(a/c)+F_2\sin\beta$	Perez et al., 1990

Finally, as evident from the GTI decomposition, the sensitivity of GTI estimates to transposition model choice or albedo assumptions lies entirely in the diffuse terms. For this reason, our analysis focuses on the tilted diffuse irradiance DTI = $G_{dh}r_d$ + $G_h\rho_g(1 - \cos\beta)/2$, sum of the sky diffuse and ground reflected components.

3. Methodology

3.1. Site, measurements and datasets

The database for this work is from the National Renewable Energy Laboratory (NREL) site in Golden, Colorado (1829 m AMSL; 39.74° N, 105.18° W) (Andreas and Stoffel, 1981). Two years of data, including GHI, DHI, DNI, GTI at a 40° tilt facing due south and shortwave surface albedo were used in this analysis, spanning a period from 1/1/2020 to 31/12/2022.

Measurements were taken with class A instruments, periodically calibrated and maintained by NREL. The one-minute resolution data was quality-controlled using the filters recommended by Perez-Astudillo et al. (2018), in order to remove outliers and inconsistent values before aggregation to hourly resolution. Table 2 summarizes the variables, instruments and number of hourly available records for each dataset.

3.2. Processing of albedo data

A simple filtering was applied to the hourly albedo measurements, removing unrealistic events where $\rho_g < 0.05$ and $\rho_g > 1$. This filtering discards 36 and 12 hourly measurements respectively, resulting on a time series of albedo shown in Figure 1. A daily series is thus derived, by averaging the hourly data for solar elevations above 10°, in order to avoid cosine response errors.

Table 2: Summary of radiometric instruments, measured variables, and data availability for the Golden, CO site from 1/1/2020 to 31/12/2021. All radiometers are manufactured by Kipp & Zonen.

Variable	Instrument	Model/Type	Hourly records
GHI	Pyranometer	CMP22	7020
DHI	Pyranometer w/shading ball	CM22	7021
DNI	Pyrheliometer	CHP1	6947
GTI 40	Tilted pyranometer	CMP22	7320
Albedo	Albedometer (up-down pair)	CMP11	8773

The albedo series exhibit marked variability throughout the analyzed period, with several episodes of high-albedo values linked to snow cover mainly during winter months. The mean albedo for the entire 2020–2021 period is 0.25. When excluding snow events ($\rho_g > 0.3$), the mean decreases to 0.20, which is consistent with the typical value reported for grass-covered surfaces without snow.

To analyze the influence of surface reflectance on the transposition models, the albedo measurements were classified into different datasets according to their temporal resolution and snow conditions, resulting in five albedo datasets: (1) a constant value of $\rho_g = 0.2$, representative of typical grass-covered surfaces without snow; (2) the hourly albedo for all conditions; (3) the daily albedo including all days, (4) the daily albedo excluding high-albedo (typically snow) events, i.e $\rho_g < 0.3$ and (5) the daily high-albedo subset of events where $\rho_g > 0.3$. These datasets were subsequently used to evaluate performance of the transposition models.

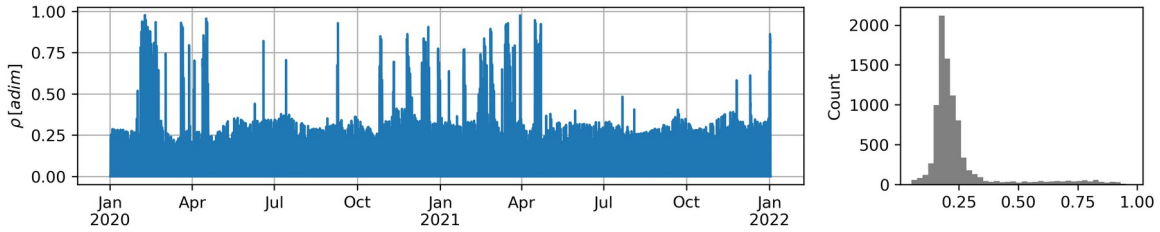

Figure 1: Time series of hourly albedo after filtering and histogram, showing the typical average of 0.2 for grass covered surfaces.

The uncertainty of each model was quantified for the five categories of albedo data by the mean bias deviation and root mean square deviation metrics, defined for a set of N measurements y_i and their estimates $\hat{y}_i$ as:

$$\text{MBD} = \frac{1}{N}\sqrt{\sum_{i}^{N}\left(\hat{y}_i - y_i\right)} \qquad \text{(eq. 2)}$$

$$\text{RMSD} = \frac{1}{N}\sqrt{\sum_{i}^{N}\left(\hat{y}_i^{\,2} - y_i^{\,2}\right)} \qquad \text{(eq. 3)}$$

Results are expressed through the relative mean bias deviation (rMBD) and the relative root mean square deviation (rRMSD), computed by normalizing the corresponding absolute metrics by the mean value of the measured DTI. An overall indicator U95 is defined as (Habte et al. (2017))

$$U_{95} = \sqrt{\left(U_{meas}\right)^2 + rRMSD^2 + rMBD^2} \qquad \text{(eq. 4)}$$

where U_{meas} is the estimated measurement uncertainty which we set as 3% of the measured mean DTI. U_{95} provides a 95% confidence interval (two standard deviations assuming a normal distribution of the residuals) for the DTI estimation and, more importantly, is useful as a unified performance indicator for model accuracy.

This analysis aims to provide a consistent framework to benchmark the performance of the five transposition models under different albedo datasets, allowing a direct comparison of their overall accuracy through the

unified U95 metric. In the following subsection, we extend this evaluation by examining the sensitivity of these performance indicators to the albedo assumptions, assessing how variations in surface reflectance influence model reliability.

3.3. Assessment of the sensitivity of metrics to albedo variations

To assess the sensitivity of the transposition models to the surface albedo, we evaluated their performance in terms of the U_{95} metric for a set of constant albedo values ranging from 0.05 to 0.9, representative of typical ground conditions from dark soil to snow. The resulting $U_{95}(\rho)$ curve provides insight into how deviations in the assumed albedo propagate into DTI estimation errors. The robustness of each model to albedo assumptions was quantified through the concavity

$$C = \frac{\partial^2 U_{95}}{\partial \rho^2} \qquad \text{(eq. 5)}$$

evaluated at the minimum of the $U_{95}(\rho)$ curve, denoted as ρ_{min}. A smaller value of C indicates that the model is less sensitive to variations in albedo, i.e., that its performance remains more stable across a broad range of surface reflectances.

The analysis was carried out both on the complete dataset, including all events with varying albedo, and separately on subsets defined by surface reflectivity, specifically events with $\rho_g < 0.3$ and $\rho_g > 0.3$. This approach allows evaluating the influence of high-albedo conditions on model performance and robustness, and ensures that sensitivity to surface reflectance is appropriately characterized.

4. Results

4.1. Model benchmarking for different albedo configurations

As an initial benchmark, the five transposition models were evaluated by calculating rRMSD, rMBD and U_{95} (Equations 2, 3 and 4) for the five categories of albedo data described in Section 3.2. The results are shown in Table 3, together with Figures 2 and 3, which are dispersion plots for the Daily-All and Snow categories of albedo (embedded in these plots we show the respective rMBD and rMSD).

Results from Table 3 and Figure 2 highlight clear differences among the models: the isotropic model has significant negative bias and high dispersion (due to its underestimation of circumsolar and horizon brightening components of sky irradiance), while the HD and HDKR models, which take into account these effects, have smaller biases and improved accuracy. The best overall performance, as measured by U_{95}, is observed for the TCK and PER models, which exhibit small biases and reduced dispersions. These results are as expected, according to their nature discussed in Section 2.

Table 3. Combined uncertainty (U_{95}, %) of the five transposition models under different albedo datasets, for the DTI component. ***($U_{95} = \sqrt{(U\_meas^2 + rRMSD^2 + rMBD^2)}$, with U_meas = 3%).*** **Mean of DTI reported in W/m²**

model	ρ_g = 0.2 constant	Daily–All	Daily–No Snow ($\rho_g < 0.3$)	Hourly	Daily - Snow ($\rho_g > 0.3$)
iso	26.2	24.2	23.8	24.5	25.0
hd	14.9	13.8	13.6	14.6	18.0
hdkr	14.0	12.9	12.7	13.8	17.9
tck	11.8	10.3	10.1	11.3	15.9
per	12.0	11.0	10.9	12.0	17.4
DTI_{mean}	176.0	176.0	173.3	176.0	196.1
records	6426	6426	5668	6426	758

Comparison through different albedo configurations show that all models have consistent relative behavior, with the TCK model performing better in all scenarios. The results also reveal that using temporally resolved albedo (daily or hourly) systematically improves accuracy with respect to a constant assumption ($\rho_g = 0.2$),

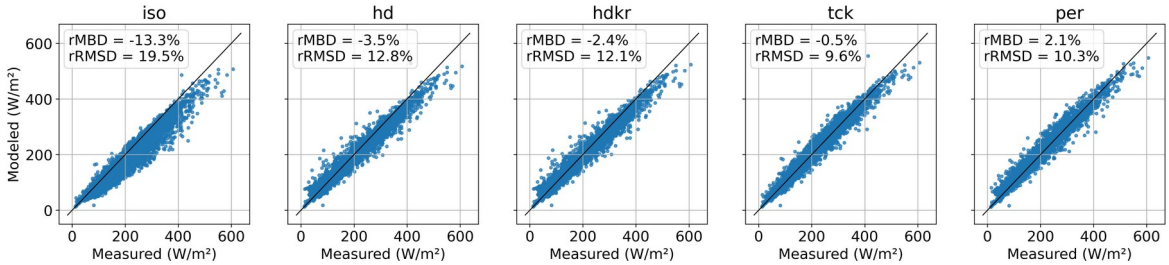

Figure 2: Comparison between modeled and measured hourly DTI, using the daily albedo series for all conditions. The mean DTI was 173.6 W/m²

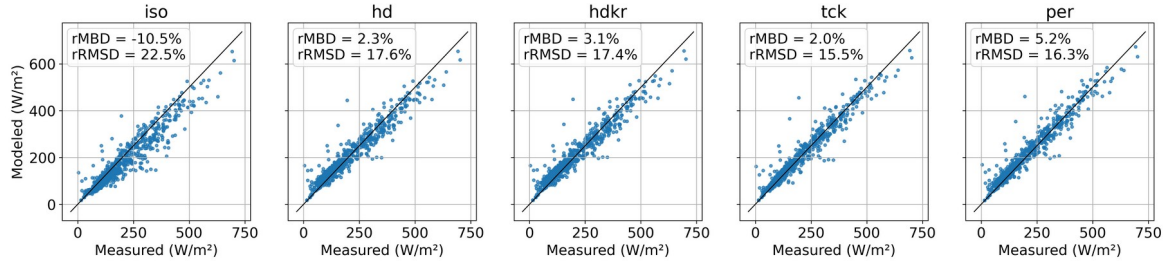

Figure 3: Comparison between modeled and measured hourly DTI, using the daily albedo series for snow conditions (ρ>0.3). The mean DTI was 196.1 W/m²

confirming the benefit of accounting for surface reflectance variability. The effect of filtering out snow events slightly lowers U_{95} for all models. Conversely, the snow subset ($\rho_g > 0.3$) shows a marked degradation in accuracy, particularly for HD and HDKR, with U_{95} increases of about 30–40 % relative to the no-snow cases.

The poorer performance of the models under snow-covered conditions can be primarily explained by the strong anisotropy of snow reflectance. Snow surfaces are highly reflective and exhibit non-Lambertian behavior, with angular variations dependent of grain size, aging, and compaction. Since most transposition models assume an isotropic (Lambertian) ground reflector, they cannot accurately reproduce the directionality of the reflected irradiance under these conditions. This effect is relevant since snow albedo can reach values above 0.8, with high variability during the day. Another factor to take into account is the fact that the albedo measurement is the result of two simultaneous irradiance measurements, with a natural propagation of the uncertainty, which coupled with the high value of albedo could be a source of error in the measurement under snow conditions.

Overall, these results indicate that model performance is largely robust to moderate albedo fluctuations, but deteriorates substantially under high-albedo conditions, emphasizing the relevance of properly representing snow-covered surfaces.

4.2. Sensitivity of model accuracy to albedo variations

Next, a sensitivity analysis was performed to examine how the unified uncertainty (U_{95}) varies with albedo, allowing us to assess each model's robustness and its response to surface reflectance assumptions. Figure 4 shows the plots of $U_{95}=f(\rho)$ for the three main scenarios: all data, filtering snow events, and the snow subset ($\rho_g > 0.3$).

The analysis of $U_{95}=f(\rho)$ reveals a consistent pattern across all scenarios. The TCK and PER models exhibit the lowest uncertainties around typical albedo values ($\approx$ 0.25), but they show significant sensitivity to deviations from the assumed albedo. In fact, their uncertainty becomes larger than that of the ISO model for assumed albedo values above 0.5. Notably, the minimum U_{95} for the TCK model occurs near the mean observed albedo, particularly in the "all" and "no-snow" cases, suggesting that its parametrization aligns well with the prevailing surface reflectance. In contrast, the ISO model shows poor performance, with both higher uncertainties and unrealistic optimal albedo values (ρ_{min} at large ρ_g). Under snow conditions, the variability of U_{95} with albedo decreases markedly (lower concavity), reflecting reduced sensitivity to albedo changes, though overall uncertainties increase and the performance gap between models (except ISO) narrows.

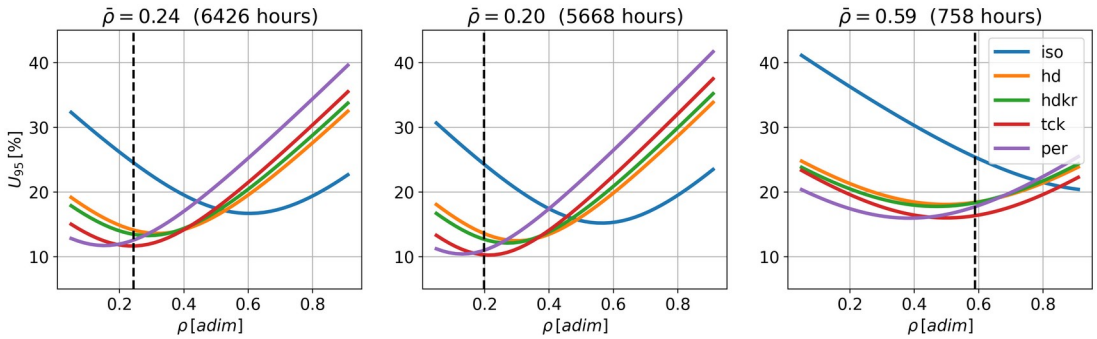

Figure 4: U_{95} as a function of albedo for three different scenarios, left: all data; middle: events without snow; right: events of snow (rho>0.3). Vertical lines show the mean value of albedo for the scenario.

4.3 Quantification of robustness

As mentioned in Section 3.3, we condense the sensitivity results from the plots in Figure 4 into a simple quantitative indicator of robustness given by the concavity C (second derivative) of the function $U_{95} = f(\rho)$ evaluated at the albedo that minimizes it, namely ρ_{min} (Equation 5). Figure 5 shows the plot of the second derivative as a function of albedo for the Daily-All set.

The PER and TCK models exhibit the sharpest and highest peaks near their respective ρ_{min}, indicating strong sensitivity to albedo assumptions and thus lower robustness. In contrast, the HD and HDKR models show broader, flatter curves, consistent with more stable behavior under varying albedo. The ISO model displays a distinct, wider distribution displaced toward higher ρ_{min}, reflecting its reduced sensitivity but generally poor overall performance.

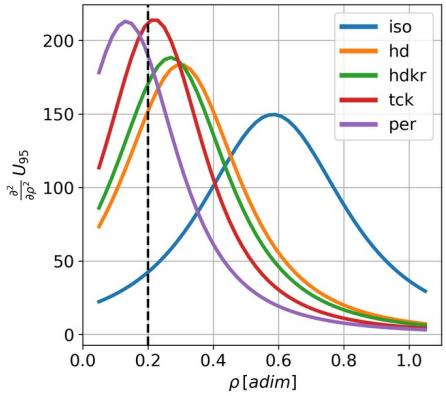

Figure 5: Second derivative of the U_{95} metric, related to the sensitivity of models to albedo assumptions. Vertical line represents the constant 0.2 reference albedo.

The results in terms of the concavity parameter are summarized in Table 4, and show that PER and TCK are the least robust models, meaning that small deviations from the true albedo can lead to large changes in uncertainty. The HD and HDKR models exhibit smaller and similar concavities, making them more robust to albedo assumptions. Although the ISO model yields the lowest C values, its overall uncertainty remain unacceptably high due to its systematic underestimation of the diffuse component of GTI.

5. Conclusions

This study evaluated the performance and robustness of five transposition models used to estimate the diffuse component (DTI) of GTI under varying surface albedo conditions, given their importance for solar energy applications. Two years of high-quality measurements from Golden, Colorado, were quality-controlled and aggregated to the hourly scale for analysis. The assessment included benchmarking using uncertainty metrics (rRMSD, rMBD, and U_{95}), a sensitivity analysis across a range of constant albedo assumptions to derive the function $U_{95} = f(\rho)$, and finally the quantification of model robustness through the concavity C of this function under snow and snow-free conditions.

Table 4: Uncertainties of the models, together with ρ_{min} and the second derivative of the U_{95} evaluated at ρ_{min}. All quantities are dimensionless.

	Daily - all			Daily - no snow			Daily - Snow		
Model	ρ_{min}	U_{95}	**C**	ρ_{min}	**U95**	**C**	ρ_{min}	U_{95}	**C**
iso	0.61	16.7	148.3	0.57	15.2	174.4	0.99	20.1	70.9
hd	0.31	13.6	183.2	0.31	12.5	210.7	0.49	18.1	78.9
hdkr	0.29	13.2	186.7	0.27	12.1	219.3	0.47	17.7	80.1
tck	0.23	11.6	213.6	0.21	10.2	258.6	0.49	16.0	89.2
per	0.15	11.7	211.5	0.13	10.4	253.7	0.39	15.9	89.0

Results show that the TCK model performs best across all albedo configurations, followed closely by PER. HDKR and HD achieve similar yet lower performance, while ISO consistently yields the highest uncertainties. This hierarchy aligns with the level of physical realism and anisotropy treatment in each model. All models perform better when using daily averaged albedo, particularly when excluding snow events ($\rho_g > 0.3$), due to reduced variability from transient surface and sensor effects. This improvement reflects noise smoothing rather than greater physical accuracy. Assuming a constant albedo of 0.2 produces only a slight degradation, validating its use when only general surface information is available. Conversely, snow-covered conditions (high ρ_g) degrade performance across all models, reflecting both anisotropic snow reflectance and high uncertainty in albedo measurements.

The analysis of $U_{95} = f(\rho)$ confirms these findings: TCK and PER achieve the lowest uncertainties near the mean observed albedo, while HD and HDKR remain more stable as assumed albedo deviates from reality. Thus, TCK and PER are preferable when reliable albedo data exist, whereas HDKR is more suitable when such data is scarce. Robustness analysis via concavity C shows PER and TCK are most sensitive to albedo deviations, while HD and HDKR are more stable; ISO, though mathematically robust, is physically unreliable due to its diffuse underestimation.

These results have direct implications in photovoltaic performance modeling under heterogeneous or variable surface conditions. Since transposition model uncertainties directly propagate to energy yield estimates, using advanced models (TCK, PER) can significantly reduce risk when albedo is well characterized. When reflectance data are uncertain or unavailable, HDKR offers an optimal balance between simplicity and robustness. This underscores the need for accurate surface optical characterization, especially in environments with snow or strong seasonal variability.

This study was limited to one site and two years of data, which may constrain generalization to other climatic or radiative contexts. Further work should extend the analysis to multi-site datasets, explore spectral and angular dependencies of albedo, and integrate satellite or model-based albedo products.

In summary, this work provides a comprehensive evaluation of transposition model performance and robustness under varying surface albedo conditions. It identifies the trade-offs between model accuracy, robustness, and data availability, offering practical guidance for both research and applied solar engineering. Beyond its immediate findings, this study contributes to the understanding of how ground reflectance interacts with diffuse irradiance modeling, an aspect that remains crucial for improving the reliability of solar resource assessment and, ultimately, for supporting the sustainable expansion of solar energy systems.

6. Aknowledgements

The authors acknowledge the technicians and experts who collected and curated the data from NREL site. We also express our gratitude to the Universidad de la República (Udelar) for its continued support and acknowledge the Comisión Sectorial de Investigación Científica (CSIC) for its support through the CSIC Grupos program.

7. References

Andreas, A., Stoffel, T., 1981. NREL Solar Radiation Research Laboratory (SRRL): Baseline Measurement System (BMS); Golden, Colorado (Data); NREL Report No. DA-5500-56488.

Duffie, J.A., Beckman, W.A., 2013. *Solar Engineering of Thermal Processes*, fourth ed. Wiley, Hoboken, NJ. https://doi.org/10.1002/9781118671603

Gueymard, C., 2008. From global horizontal to global tilted irradiance: How accurate are solar energy engineering predictions in practice? *Proceedings of Solar 2008 Conference*, San Diego, CA, American Solar Energy Society.

Habte, A., Sengupta, M., Lopez, A., 2017. Evaluation of the National Solar Radiation Database (NSRDB Version 2): 1998–2015. Technical Report NREL/TP-5D00-67722, National Renewable Energy Laboratory, Golden, CO.

Hay, J.E., Davies, J.A., 1980. Calculation of the solar radiation incident on an inclined surface. In: Hay, J., Won, T. (Eds.), *First Canadian Solar Radiation Data Workshop*. Atmospheric Environment Service, pp. 59–72.

Klucher, T.M., 1979. Evaluation of models to predict insolation on tilted surfaces. *Solar Energy* 23(2), 111–114. https://doi.org/10.1016/0038-092X(79)90110-5

Liu, B.Y.H., Jordan, R.C., 1961. Daily insolation on surfaces tilted towards the equator. ASHRAE Journal, 10, 53–59. https://www.osti.gov/biblio/5047843

Perez, R., Ineichen, P., Seals, R., Michalsky, J., Stewart, R., 1990. Modeling daylight availability and irradiance components from direct and global irradiance. *Solar Energy* 44, 271–289. https://doi.org/10.1016/0038-092X(90)90055-H

Perez-Astudillo, D. et al., 2018. Improved quality control protocols on solar radiation measurements. Solar Energy, 169, 425-433. https://doi.org/https://doi.org/10.1016/j.solener.2018.05.028

Reindl, D.T., Beckman, W.A., Duffie, J.A., 1990. Evaluation of hourly tilted surface radiation models. *Solar Energy* 45(1), 9–17. https://doi.org/10.1016/0038-092X(90)90061-G

Temps, R., Coulson, K., 1977. Solar radiation incident upon slopes of different orientations. *Solar Energy* 19(2), 179–184. https://doi.org/10.1016/0038-092X(77)90056-1

Tuomiranta, A. et al., 2021. Worldwide performance evaluation of ground surface reflectance models. Solar Energy, 224, 1063-1078. https://doi.org/https://doi.org/10.1016/j.solener.2021.06.023

Yang, D., 2016. Solar radiation on inclined surfaces: Corrections and benchmarks. Solar Energy, 136. 288-302. https://doi.org/https://doi.org/10.1016/j.solener.2016.06.062